Ain Shams Engineering Journal 16 (2025) 103604

Contents lists available at ScienceDirect

Ain Shams Engineering Journal

journal homepage: www.sciencedirect.com

Full Length Article

Modeling information and communication interaction in 5G cluster considering the variability of the base station coverage zone

Viacheslav Kovtun [a,*], Oksana Kovtun [b], Jamil Abedalrahim Jamil Alsayaydeh [c]

[a] Internet of Things Group, Institute of Theoretical and Applied Informatics Polish Academy of Sciences, Bałtycka 5, 44-100 Gliwice, Poland
[b] Department of the Theory and Practice of Translation, Faculty of Foreign Languages, Vasyl' Stus Donetsk National University, 600-Richchya Str., 21, 21000 Vinnytsia, Ukraine
[c] Department of Engineering Technology, Fakulti Teknologi and Kejuruteraan Elektronik and Komputer (FTKEK), Universiti Teknikal Malaysia Melaka, Durian Tunggal (UTeM), Melaka 76100, Malaysia

ARTICLE INFO

Keywords:
Information and communication interaction
5G cluster
Coverage area segmentation
Mobile subscribers
Communication performance
Multi-line queuing system
Qualitative metrics

ABSTRACT

The research focuses on the processes of information and communication interaction between a set of subscribers and a base station in a 5G cluster. We consider that the coverage area of the latter is divided into concentric segments relative to the location of the base station. Each concentric segment is characterized by the distance to the center of the 5G cluster, the presence of opaque obstacles in the radio signal propagation path, and the service speed of subscribers within its boundaries. A multi-line queuing system without the buffer is chosen as the model of the researched process. The parameters of this system, including the incoming request flow and the process of servicing them, are determined by a set of states of an external stochastic process that characterizes the variability of the coverage area of the base station in the 5G cluster. The incoming request flow is represented by a marked Markovian point process, allowing for the typification of requests by the index of the segments of their origin. We consider that during the information and communication interaction process, a subscriber may move between segments of the 5G cluster as well as leave its boundaries (handover type). For the described multi-dimensional Markovian chain of the queuing system, the stationary probabilities of its states are analytically formalized. The obtained expressions are generalized to metrics of qualitative indicators aimed at characterizing the performance of the target instance of the 5G cluster. The results of the experiments demonstrated the sensitivity of the proposed qualitative parameters to both variations in the number of available channels to subscribers in the target 5G cluster and to the consideration of the variability aspect of the coverage area of the base station. An example of formulating optimization tasks for the performance of the target 5G cluster based on the proposed metrics of qualitative indicators is provided.

1. Introduction and state-of-the-art

1.1. Relevance of the research

In modern cellular networks of the 5G generation and beyond, the dominant traffic is not voice but rather streaming multimedia [1]. Due to this circumstance, the use of classical approaches from teletraffic theory [2,3] to assess the performance characteristics of designed 5G clusters as basic elements of cellular networks appears insufficient. Specifically, when estimating the necessary amount of logical channels with guaranteed data traffic rates, it is necessary to consider the potential for dynamically altering the modulation scheme to meet the requirements of Quality of Service (QoS) policies [4,5].

The outcome of the aforementioned scheme selection procedure is ensured, in part, by the quality characteristics of the wireless communication channel used to implement the information exchange between the target subscriber and the base station in the 5G cluster. The quality of the wireless communication channel depends on several factors [6], the most notable of which are the distance between the target subscriber and the base station, as well as the presence of radio-opaque obstacles in the path of the information signal propagation. The complexity of accounting for these factors is compounded when considering that subscribers may move both within the 5G cluster and outside its boundaries.

Finally, it should be noted that the characteristics of the incoming request flow from subscribers in a 5G cluster cannot strictly be considered constant. Service rates for requests in a 5G cluster depend on the

* Corresponding author.
E-mail addresses: kovtun_v_v@vntu.edu.ua (V. Kovtun), o.kovtun@donnu.edu.ua (O. Kovtun), jamil@utem.edu.my (J.A. Jamil Alsayaydeh).

https://doi.org/10.1016/j.asej.2025.103604
Received 5 June 2024; Received in revised form 9 April 2025; Accepted 24 June 2025
Available online 19 July 2025

potentially changing locations of subscribers relative to the cluster center. In many typical high-load 5G clusters [7–9], these characteristics may vary depending, for instance, on the time of day, the accessibility of network resources, channel interference, etc. It is promising to generalize these distorting factors in the format of an external (relative to the processes of information and communication interaction) stochastic flow, which determines the variability of the coverage area of the base station. Based on the arguments presented, the authors consider a rigorous analytical formalization of the influence of this flow on the information and communication processes in the target 5G cluster as a promising research task.

1.2. State-of-the-art

Recent studies have scrutinized a 5G networks performance in city and rural settings [10–12]. Paper [13] provided a succinct analysis of 5G wireless networks, focusing on key metrics such as throughput and latency, while also discussing enhancements like carrier aggregation and network slicing. Study [14] conducted a thorough analysis using ray tracing simulations to evaluate 5G NR coverage in urban areas. They highlighted the unique challenges posed by urban environments, such as buildings and clutter affecting signal paths, crucial for successful deployment. Work [15] analyzed 5G communication performance, noting a decrease in performance with distance but still meeting most application requirements.

Research [16] delved into the intricacies of attaining broad access to 5G networks across various city and rural terrains. They emphasized the challenges stemming from varying infrastructure requirements, subscribers' density fluctuations, and spectrum allocation strategies. To tackle these hurdles, the authors proposed a thorough strategy involving network densification, efficient spectrum management, and cost-effective deployment methods. They underscored the importance of tailoring network remedies to fit the distinct requirements of each setting, whether densely populated city areas or sparsely inhabited rural regions. Meanwhile, [17] carried out a comparative investigation of different millimeter-wave bands within 5G networks, analyzing factors like path attenuation and penetration. They underscored the trade-offs between frequency bands and their suitability across varied deployment scenarios.

Numerous investigations have focused on assessing 5G efficiency in real-world settings. A study [18] assessed the functionality of a 5G device in a private network, noting its ability to achieve high data transfer rates while keeping latency minimal. Nevertheless, they noticed that the device's functionality was susceptible to factors like network overcrowding and interference. Meanwhile, [19] investigated the functionality of 5G millimeter-wave radio access in terms of delay in outdoor mobile settings and beam tracking. Their results underscored the significant latency performance improvement achievable through beam tracking, particularly in scenarios lacking direct line of sight.

Article [20] undertook an exhaustive analysis of critical performance metrics in 5G networks, centering on network structure. Their research introduces innovative optimization approaches and methodologies, including network slicing and resource control algorithms. Employing mathematical modelling, they meticulously assessed these methods, showcasing significant improvements in network efficiency compared to traditional, unoptimized setups.

Work [21] suggested a flexible system customized for cross-network monitoring of end-to-end assurances within private 5G networks. Employing a distributed test environment, they revealed a method actively measuring latency, throughput, and reliability across various network nodes, providing a comprehensive evaluation exceeding traditional single-point assessments. This methodology proves particularly valuable for scenarios involving multiple users and edge circumstances, where performance fluctuation is more pronounced.

Lastly, [22] undertook a systematic examination of 5G technology, concentrating on key-performance indicators (KPIs) and assessing its efficiency. They identified key metrics such as reliability, latency, throughput,' and energy efficiency, emphasizing continuing investigation endeavors aimed at fully comprehending 5G efficiency across various subscriber conditions and deployment scenarios.

The literature has extensively examined how subscribers' mobility can enhance 5G cluster performance, as evidenced by several studies [23–27]. These papers predominantly delve into theoretical aspects and performance boundaries. For instance, [23] delineates two limit scenarios of extremely rapid and exceedingly slow channel variations, demonstrating their utility in establishing straightforward bounds on flow-level performance. Research [24] contributes by establishing both lower and upper bounds for flow-level performance metrics, illustrating that mobility generally augments network capacity.

Work [25] investigates networks featuring multiple interacting base stations, concluding that mobility expands the stability region of the system. Additionally, Article [26] employs a multi-dimensional Markovian chain to model an OFDMA system integrating Proportional Fairness (PF) and Hierarchical Modulation (HM), revealing that, in the presence of HM, simple cyclic services like Round Robin outperform PF. Notably, [27] scrutinizes the influence of subscribers' mobility on cell performance under fair and opportunistic scheduling schemes. The findings highlight that mobility enhances throughput performance, particularly at the cell edge. However, due to the non-reversibility of the associated Markovian process in scenarios where mobile users equitably share resources, [28] can only derive closed-form expressions in two extreme cases: when subscribers are stationary and when they theoretically possess infinite speed. Consequently, for more realistic speeds, their analysis necessitates the numerical solution of multi-dimensional Markovian chains.

A common drawback of the mentioned studies is that they do not consider the parameters characterizing the input request flow from potentially mobile subscribers, service rates for accepted requests, and other characteristic parameters of the models changing over time. As we have already mentioned in Section 1, in many real cellular networks, these parameters vary significantly and discontinuously. A practical way to adequately account for such dependencies is to investigate corresponding models considering the random environment in which they operate. By a random environment, we mean some external random process, such as a Markovian chain with a finite state space. All or some parameters of the investigated model are perceived as dependent on the state of this chain and change discontinuously, reacting to its dynamics. In our article, we explore the performance of a 5G cluster model operating in a random environment, taking into account the dependency of the input request flow parameters and the service process on the locations of potentially mobile subscribers within the coverage area of the base station.

Additionally, recent studies have addressed the performance modelling of 5G networks from various perspectives. For example, Chen et al. [29] developed an analytical framework for ultra-reliable low-latency communication (URLLC), focusing on physical-layer metrics such as delay and packet error probability under finite blocklength constraints. Their approach is effective for low-latency analysis but does not consider spatial coverage dynamics or sector-based queueing interactions. In another study, Zhu et al. [30] examined user-centric clustering in dense 5G networks using tools of stochastic geometry, highlighting spatial user distribution but omitting temporal fluctuations in service dynamics and queuing behaviour. In contrast, the present work proposes a hybrid analytical model that integrates a two-state external stochastic process – governing the dynamic reconfiguration of the base station's coverage area—with a multidimensional Markovian queueing system that captures sector-specific traffic and service transitions. The availability of closed-form performance expressions further distinguishes our approach, enabling analytically grounded evaluation of blocking probability, service intensity, and load distribution in dynamically evolving 5G-IoT clusters.

To improve the transparency and consistency of the mathematical notations used throughout the manuscript, we provide a summary of the key parameters, variables, and symbols in Table 1.

1.3. Main attributes of the research

Let's summarize the characteristic information about the article by formulating the object, subject, goal, tasks, and main contribution of the research.

The object of the research is the multi-line process of information and communication interaction between a set of subscribers and a base station in a 5G cluster.

The subject of the research is the elements of teletraffic theory, queuing theory, renewal theory, probability theory, and mathematical statistics.

The goal of the research is to formalize metrics of qualitative indicators for evaluating the performance of the model of a 5G cluster target instance, where the flow of incoming requests and the process of servicing them are determined by a set of states of an external stochastic process characterizing the variability of the coverage area of the base station.

To achieve the set goal, the following research tasks were performed:

– The investigated process was adequately represented in the formalism of queuing theory (Section 2.1).

– The functioning process of the obtained queuing system was described using a multidimensional Markovian chain, and computationally efficient information technology for determining its stationary distribution was formulated (Section 2.2).

– Based on the defined characteristics of the stationary distribution of the research object model, a metric of qualitative indicators was analytically formalized to characterize the performance of the target instance of the 5G cluster (Section 2.3).

– The adequacy of the presented mathematical apparatus was empirically demonstrated, and the significance of the variability of the coverage area of the base station on the performance of the 5G cluster was demonstrated through examples.

Finally, let's formulate the main contribution of the research. By modeling the research object, we take into account that the coverage area of the 5G cluster is divided into concentric segments relative to the base station's location. Each such concentric segment is characterized by the distance to the center of the 5G cluster, the opaque interference presence along the radio signal propagation path, and the service rate of subscribers within its boundaries. These specific features of the research object are considered in the created multi-line queuing system without the buffer. The parameters of this system, including the characteristics of the incoming request flow and the servicing process, are not considered constant (as in potential analogs of our research) but are determined by a set of states of an external stochastic process that characterizes the variability of the coverage area of the base station in the 5G cluster. We represent the incoming request flow as a marked Markovian point process. This allows us to take into account the typification of requests by the index of segments of their origin. We consider that during the information and communication interaction process, a subscriber can both move between segments of the 5G cluster and leave its boundaries (handover type). For the described multidimensional Markovian chain of the queuing system, stationary probabilities of its states are analytically formalized. The obtained expressions are generalized to the metric of qualitative indicators aimed at characterizing the performance of the target instance of the 5G cluster.

Table 1
Key Notations Used in the Mathematical Model.

Symbol	Description
λ	Total arrival rate of input requests to the system
η	Intensity of the external stochastic process influencing coverage dynamics
K	Number of concentric coverage segments in the adaptive zone
η_i	Arrival intensity of requests originating from segment ii
μ_i	Service rate of requests from segment ii
θ_i	Rate of transition (mobility) between coverage segments
$R(t)$	Time-varying radius of the adaptive coverage zone
N	Total number of subscriber devices in the system
S	Set of states in the Markov model
$s \in S$	Index of a concentric sector (coverage segment number)
ν	Unit vector of appropriate dimension (used in block structure definitions)
ρ	Stationary distribution of the control process tata
h	Absorbing state in the service process tμtμ, corresponding to handover
Π	Transition intensity matrix of the service process t_μ
$\widetilde{P}_{ij}$	Transition probability from state ii to jj in the reduced chain
$\widetilde{b}_{ij}$	Element of the sub-generator matrix for rejection (blocked) states
$\overrightarrow{P}$	Infinitesimal generator matrix of the main Markov process
$\overrightarrow{\pi}$	Stationary distribution vector (notation introduced for general reference)
(n,i)	Discrete state: n active requests in segment i
tilde ($\widetilde{\cdot}$) notation	Indicates reduced or modified quantities (e.g., conditioned sub-processes)
arrows ($\overrightarrow{\cdot}$)	Denote vectors or structured matrices
lowercase letters	Scalar parameters or indices
capital letters	Sets, matrices, or state identifiers

2. Models and methods

2.1. Statement of the research

Let's assume that a 5G cluster is confined to the coverage area of a base station capable of guaranteed servicing K subscriber devices simultaneously. According to the objective speed of such a service, the coverage area is segmented into $S \in \mathbb{N}$ concentric sectors. Each $s-$th sector, $s \in \{\overline{1,S}\}$, differs in distance from the 5G base station and the opaque interference presence on the radio signal propagation path. We consider that during active informational interaction with the base station, the subscriber may both move between sectors and leave the boundaries of the 5G cluster altogether. In this case, we will categorize incoming requests according to the segment index in which the subscriber's device was located at the time of communication with the base station.

As the basic model for the 5G cluster, we will use a $K-$linear queueing system without a buffer. In this regard, we take into account that the parameters of this system, including the input request flow and the process of servicing them, are determined by the set of states of an external stochastic process n_t, $t \geqslant 0$, which characterizes the variability of the coverage area of the 5G cluster's base station. We interpret n_t as an unnormalized continuous Markovian chain with an infinitesimal generator G and a phase space $\{\overline{1,N}\}$. We consider the flow of typed incoming requests as a marked Markovian point process, which allows us to take into account the aspect of typing of the first ones. We will describe the arrival times of incoming requests as a continuous Markovian process a_t, $t \geqslant 0$, with a phase space $\{\overline{1,A}\}$. Therefore, we characterize the input request flow with a two-dimensional continuous Markovian chain $\{n_t, a_t\}$, $t \geqslant 0$.

At the state $n \in \{\overline{1,N}\}$ of process n_t, the flow of typed incoming requests is characterized by a set of square matrices $\left\{B_0^{(n)}, \ldots, B_s^{(n)}\right\}$, $s = \overline{1,S}$. Generalized by matrix $B_s^{(n)}$, the elements represent specific registration of incoming request type $r \in \{\overline{1,R}\}$ process a_t transition intensities for the process n_t current state. Now we interpret the contents of the matrix $B_0^{(n)}$. The off-diagonal elements of this matrix characterize transition intensities of the process a_t not caused by the arrival of a typed incoming request. The diagonal elements of matrix $B_0^{(n)}$ characterize output intensities of process a_t from the corresponding states. Let's introduce the notation $B^{(n)}(1) = B_0^{(n)} + B^{(n)}$, where $B^{(n)} = \sum_{s=1}^{S} B_s^{(n)}$.

For state $n \in \{\overline{1,N}\}$ of the external process n_t, the average intensity $\eta^{(n)}$ of arrival of typed incoming requests is established as $\eta^{(n)} = B^{(n)}\widehat{\nu}\overrightarrow{\rho}^{(n)}$, where $\widehat{\nu}$ is a unit column vector of corresponding length, and the row vector $\overrightarrow{\rho}^{(n)}$ is a sole solution of the $\overrightarrow{\rho}^{(n)}B^{(n)}(1) = \overrightarrow{0}$, $\overrightarrow{\rho}^{(n)}\widehat{\nu} = 1$, system of equations, where $\overrightarrow{0}$ is a row vector of corresponding length, all elements of which are zero. In this context, for state z $n \in \{\overline{1,N}\}$ of the external process n_t, the average intensity $\eta_s^{(n)}$ of arrival of requests of type $s \in \{\overline{1,S}\}$ is determined as $\eta_s^{(n)} = B_s^{(n)}\widehat{\nu}\overrightarrow{\rho}^{(n)}$.

For the state $n \in \{\overline{1,N}\}$ of the external process n_t, the relative standard deviation $c_{\mathrm{v}}^{(n)}$ of consecutive intervals between incoming requests is determined as $c_{\mathrm{v}}^{(n)} = 2\eta^{(n)}\overrightarrow{\rho}^{(n)}\widehat{\nu}/\left(-B_0^{(n)}\right) - 1$. In turn, for state $n \in \{\overline{1,N}\}$ of the external process n_t, the correlation coefficient $c_{\mathrm{r}}^{(n)}$ for two consecutive time intervals between incoming requests is determined as $c_{\mathrm{r}}^{(n)} = \left(\frac{\eta^{(n)}\overrightarrow{\rho}^{(n)}B^{(n)}\widehat{\nu}}{\left(-B_0^{(n)}\right)^2} - 1\right)/c_\nu^n$.

We define the matrices $\left\{\widetilde{B}_s, \widetilde{B}_0, \widetilde{B}, \widetilde{B}(1)\right\}$ as $\widetilde{B}_s = diag\{B_s^{(n)}, n = \overline{1,N}\}\forall s = \overline{1,S}$, $\widetilde{B}_0 = G \otimes I_W + diag\left\{B_0^{(n)}, n = \overline{1,N}\right\}$, $\widetilde{B} = \sum_{s=1}^{S}\widetilde{B}_s$, $\widetilde{B}(1) = \widetilde{B}_0 + \widetilde{B}$, whereby the term $diag(\bullet)$ we denote a block-diagonal matrix, the diagonal blocks of which are listed in parentheses; by the symbol $\otimes$ we denote the Kronecker product.

In the context of $\left\{\widetilde{B}_s, \widetilde{B}_0, \widetilde{B}, \widetilde{B}(1)\right\}$, let's redefine the expressions characterizing the average intensity of the input flow η and the intensity η_s of arrival of incoming requests of the s−th type:

$$\eta = \overrightarrow{\rho}\widetilde{B}\widehat{\nu}\eta_s = \overrightarrow{\rho}\widetilde{B}_s\widehat{\nu}s = \overline{1,S} \tag{1}$$

where the vector $\overrightarrow{\rho}$ represents the unique solution of the system of equations $\overrightarrow{\rho}\widetilde{B}(1) = \overrightarrow{0}$, $\overrightarrow{\rho}\widehat{\nu} = 1$. Let's also define the relative standard deviation c_{v} of the durations of intervals between moments of arrival of incoming requests as $c_{\mathrm{v}} = 2\eta\overrightarrow{\rho}\widehat{\nu}/\left(-\widetilde{B}_0\right) - 1$, and the correlation coefficient c_{r} of the durations of two consecutive intervals between moments of arrival of incoming requests as $c_{\mathrm{r}} = \left(\frac{\eta\overrightarrow{\rho}\widetilde{B}\widehat{\nu}}{\left(-\widetilde{B}_0\right)^2}\right)/c_{\mathrm{v}}$.

To enhance the conceptual clarity of the proposed model, we introduce a graphical representation of the queuing system's key elements and their interactions (see Fig. 1).

The diagram captures the dynamic behaviour of mobile subscribers within an adaptive 5G coverage zone segmented into K concentric areas. Each segment is characterised by its own arrival intensity η_i, service rate μ_i, and inter-segment transition rate θ_i, while the overall system is influenced by an external stochastic process of intensity η. The adaptive radius $R(t)$ reflects the time-dependent nature of the coverage area. Each state of the system is formally defined by a pair (n, i), where n denotes the number of incoming requests in segment i. Requests are processed by a system without buffering, meaning that any excess traffic is rejected when the system is busy. This conceptual scheme also illustrates the pipeline from input request handling to stationary distribution analysis, through which performance indicators – such as blocking probability and throughput – are derived.

If an incoming request arrives when the base station is already serving K requests, then the incoming request is rejected. Otherwise, the incoming request is accepted for servicing. Given a fixed state $n \in \{\overline{1,N}\}$, the duration of a subscriber's stay, whose request originates from the s−th sector, is characterized by an exponentially distributed stochastic variable $\lambda_s^{(n)}$, $s \in \{\overline{1,S}\}$. The subscriber may leave the sector s due to:

- Completion of servicing their request;
- Moving to the sector s', accompanied by a change in the type of serviced request from s to s', respectively;
- The subscriber leaves the boundaries of the 5G cluster, accompanied by a change in the type of serviced request from s to handover h. Each of these situations is characterized by a certain probability.

Expressing the last ones through the parameter $\lambda_s^{(n)}$, let's introduce:

- The intensity of completing the servicing of a request $\lambda_{s,+}^{(n)}$,
- The intensity of changing the type of serviced request $\lambda_{s,s'}^{(n)}$,

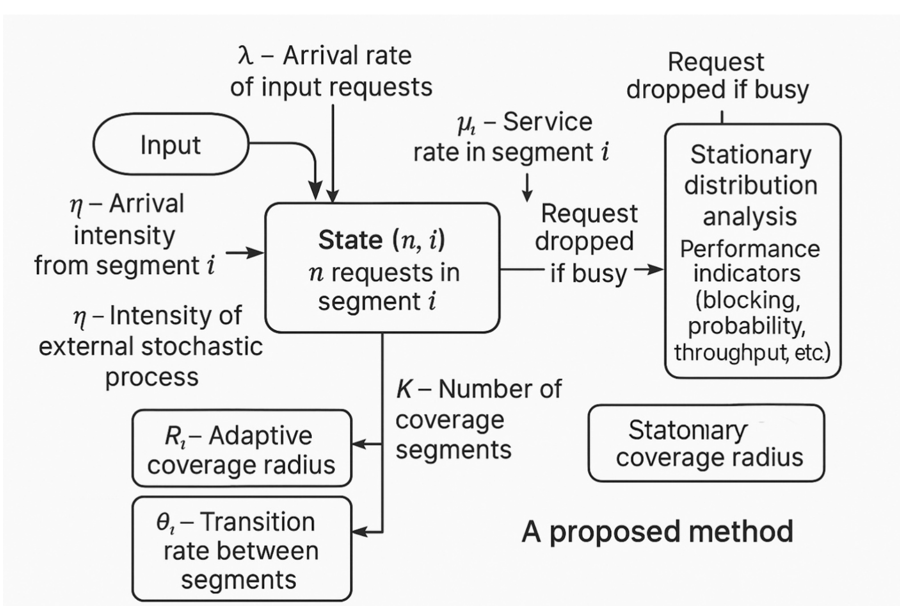

Fig. 1. Conceptual diagram of the state-based queuing model in a segmented 5G system.

– The intensity of classifying the serviced request as a handover $\lambda_{s,h}^{(n)}$.

In this case, $\lambda_s^{(n)} = \lambda_{s,+}^{(n)} + \lambda_{s,h}^{(n)} + \sum_{s'=1,s'\neq s}^{S} \lambda_{s,s'}^{(n)}$.

The complex structure of intensity $\lambda_s^{(n)}$ leads us to define the duration of servicing any request in the 5G cluster as a stochastic variable with a generalized phase-type distribution [31]. Such a choice is based on the fact that the investigated requests are heterogeneous with a differentiation of the result of their servicing. In the framework of the chosen mathematical apparatus, we interpret the duration of servicing any request in the 5G cluster as the time taken for an unnormalized Markovian chain μ_t, $t \geqslant 0$, with absorbing states $\{+, h\}$ and transient states $\{\overline{1,S}\}$, to reach one of the absorbing states. The initial state of such a chain corresponds to a type of incoming request accepted for servicing: $s \in \{\overline{1,S}\}$. For a fixed state $n \in \{\overline{1,N}\}$, the transition intensity matrix μ_t between states of process takes the form

$$\Pi^{(n)} = \begin{pmatrix} -\lambda_1^{(n)} & \lambda_{1,2}^{(n)} & \dots & \lambda_{1,S}^{(n)} \\ \lambda_{2,1}^{(n)} & -\lambda_2^{(n)} & \dots & \lambda_{2,S}^{(n)} \\ \vdots & \vdots & \ddots & \vdots \\ \lambda_{S,1}^{(n)} & \lambda_{S,2}^{(n)} & \dots & -\lambda_S^{(n)} \end{pmatrix} \tag{2}$$

The process μ_t staying in state s means that the incoming request accepted from the source originating from the $s-$th sector receives the corresponding type of servicing. When the sector of origin of the serviced request changes, the process μ_t transitions to the corresponding transient state. The transition of the process μ_t to the first absorbing state signifies the successful completion of the accepted incoming request servicing. In terms of (2), this event is characterized by the column vector components $\overrightarrow{\Pi}_+^{(n)} = \left(\lambda_{1,+}^{(n)}, \lambda_{2,+}^{(n)}, \dots, \lambda_{S,+}^{(n)}\right)^T$, where the symbol T denotes the transposition operation. Similarly, the transition of a process μ_t to the handover state is characterized by the column vector components $\overrightarrow{\Pi}_h^{(n)} = \left(\lambda_{1,h}^{(n)}, \lambda_{2,h}^{(n)}, \dots, \lambda_{S,h}^{(n)}\right)^T$. It is worth noting that the transition of a process n_t, $t \geqslant 0$, to another state does not entail a synchronous change in the states of processes a_t, μ_t, $t \geqslant 0$, but it causes changes in the intensities of their transitions.

In our study, we assume that all the parameters introduced in Section 2.1 are known and controllable. Next, we will focus on formalizing the properties of the Markovian processes $\{n_t, a_t, \mu_t\}$, $t \geqslant 0$, which characterize the dynamics of the queuing system as a model of the information and communication interaction process in the 5G cluster.

2.2. Description of the dynamics of the Markovian process of information and communication interaction in a 5G cluster

To describe the dynamics of the information and communication interaction process in a 5G cluster, let's introduce a generalized continuous-time regular non-reduced Markovian chain $\varsigma_t = \left\{k_t, n_t, a_t, \overrightarrow{l}_t\right\}$, where at time $t \geqslant 0$, parameter $k_t \in \{\overline{1,K}\}$ characterizes the number of incoming requests for service, parameter $n_t \in \{\overline{1,N}\}$ characterizes the variability of the coverage zone of the 5G base station, parameter $a_t \in \{\overline{1,A}\}$ characterizes the state of the marked Markovian point process of managing the flow of typified incoming requests, and the components of vector $\overrightarrow{l}_t = \left\{l_t^{(s)}\right\}$ characterize the number of subscribers in each $s-$th concentric sector of the coverage zone of the 5G base station, $l_t^{(s)} = \overline{0,k_t}$, $l_t^{(s)} = k_t$, $s = \overline{1,S}$.

We have constructed the Markovian chain ς_t concerning the vector $\overrightarrow{l}_t$, whose components characterize the number of subscribers in each sector of the 5G cluster coverage, rather than for the number of communication resources that the 5G base station uses to serve each incoming request. This approach significantly reduces the dimensionality of the state space and makes the model more precise regarding the task of determining the number of concentric sectors S without excessive computational resource consumption. As a result, the dimensionality of the state space of a process ς_t is such: $NA\sum_{k=0}^{K} J_k$, where $J_k = C_{k+S-1}^{S-1} = (k+S-1)!/k!(S-1)!$. We describe the stationary probabilities of states of the unreduced Markovian chain ς_t by the expression

$$q\left(k, n, a, l^{(1)}, \dots, l^{(S)}\right) = \lim_{t\to\infty} Q\{k_t = k, \\ n_t = n, a_t = a, l_t^{(1)} = l^{(1)}, \dots, l_t^{(S)} = l^{(S)}\right\},$$

where $k = \overline{0,K}$, $n = \overline{1,N}$, $a = \overline{1,A}$, $l^{(s)} = \overline{0,k}$, $\sum_{s=1}^{S} l^{(s)} = k$.

By definition, for a Markovian chain ς_t, stationary probabilities $q\left(k, n, a, l^{(1)}, \dots, l^{(S)}\right)$ exist for any values of system's parameters. We form row vectors $\overrightarrow{q}(k,n)$, $k = \overline{0,K}$, $n = \overline{1,N}$, from these probabilities by redefining probabilities $q\left(k, n, a, l^{(1)}, \dots, l^{(S)}\right)$ in the inverse lexicographic order of components $l^{(1)}, \dots, l^{(S)}$ and the direct lexicographic order of component a. Based on $\overrightarrow{q}(k,n)$, we form vectors $\overrightarrow{q}_k$, $k = \overline{0,K}$: $\overrightarrow{q}_k = (\overrightarrow{q}(k,1), \overrightarrow{q}(k,2), \dots, \overrightarrow{q}(k,N))$. As known, probability vectors $\overrightarrow{q}_k$, $k = \overline{0,K}$, satisfy a system of linear equilibrium equations $\left(\overrightarrow{q}_0, \overrightarrow{q}_1, \dots, \overrightarrow{q}_K\right) P = \overrightarrow{0}$, $\left(\overrightarrow{q}_0, \overrightarrow{q}_1, \dots, \overrightarrow{q}_K\right) \widehat{\nu} = 1$, where P is the infinitesimal generator of a Markovian chain ς_t, $t \geqslant 0$. It is this generator that needs to be determined for further calculation of the stationary probabilities of the states of the investigated system.

Let's introduce a series of notations, including: – the identity and zero matrices of corresponding dimensions: E and O, respectively; – a symbol for the Kronecker sum of matrices: $\oplus$; – matrices $\widetilde{\Pi}_1^{(n)} = \begin{pmatrix} 0 & 0 \\ \overrightarrow{\Pi}_+^{(n)} & \Pi^{(n)} \end{pmatrix}$, $\widetilde{\Pi}_2^{(n)} = \begin{pmatrix} 0 & 0 \\ \overrightarrow{\Pi}_h^{(n)} & \Pi^{(n)} \end{pmatrix}$, $n = \overline{1,N}$; – a row vector of length S, where all components are zero except the $s-$th component, which is one: $\overrightarrow{b}^{(s)}$, $s = \overline{1,S}$.

According to the Ramaswami-Lukanthony approach [32], provided that at the moment of transition of process ς_t, k requests in the 5G cluster are served: – matrix $A_k(b_s)$ characterizes a transition probabilities of process $\overrightarrow{l}_t$, $t \geqslant 0$, at the beginning of servicing by the system of an incoming request of type s; – matrix $B_{K-k}\left(K, \widetilde{\Pi}_i^{(n)}\right)$ characterizes a transition intensities of process $\overrightarrow{l}_t$ when a controlling process transitions from one of the serviced requests to an absorbing state $i=\{1,2\}$ at a fixed value of $n \in \{\overline{1,N}\}$; – matrix $\Gamma_k\left(K, \Pi^{(n)}\right)$ characterizes a transition intensities of process $\overrightarrow{l}_t$ between transient states at a fixed value of $n \in \{\overline{1,N}\}$; – the magnitudes of the diagonal elements of the diagonal matrix $D_k^{(n)}$ characterize the total intensity of the process $\overrightarrow{l}_t$ exiting from the corresponding state at a fixed value of $n \in \{\overline{1,N}\}$. On this basis, we generalize the intensities of all transitions of the Markovian chain ς_t, $t \geqslant 0$, that occurred during an infinitesimal time interval into a three-diagonal block matrix P. This infinitesimal generator for the process ς_t, $t \geqslant 0$, takes the form

$$P = \begin{pmatrix} P_{0,0} & P_{0,1} & O & O & \dots & O & O \\ P_{1,0} & P_{1,1} & P_{1,2} & O & \dots & O & O \\ O & P_{2,1} & P_{2,2} & P_{2,3} & \dots & O & O \\ \vdots & \vdots & \vdots & \vdots & \ddots & \vdots & \vdots \\ O & O & O & O & \dots & P_{K,K-1} & P_{K,K} \end{pmatrix} \tag{3}$$

The non-zero blocks of matrix (3) are defined as

$$P_{0,0} = \widetilde{B}_0 = diag\left\{B_0^{(n)}, n = \overline{1,N}\right\} + G \otimes E_A$$

$$P_{k,k} = diag\left\{B_0^{(n)} \oplus \left(\Gamma_k\left(K,\Pi^{(n)}\right) + D_k^{(n)}\right),\ n = \overline{1,N}\right\} + G \otimes E_{AJ_k}, k = \overline{1,K-1},$$

$$P_{K,K} = diag\left\{B_0^{(n)} \oplus \left(\Gamma_K\left(K,\Pi^{(n)}\right) + D_k^{(n)}\right) + B^{(n)} \otimes E_{J_K}, n = \overline{1,N}\right\} + G \otimes E_{AJ_K},$$

$$P_{k,k1} = diag\left\{E_A \otimes \left(\mathrm{B}_{K-k}\left(K,\widetilde{\Pi}_1^{(n)}\right) + \mathrm{B}_{K-k} \times \left(K,\widetilde{\Pi}_2^{(n)}\right)\right), n = \overline{1,N}\right\}, k = \overline{1,K},$$

$$P_{k,k+1} = diag\left\{\sum_{s=1}^{S} B_s^{(n)} \otimes \mathrm{A}_k(b_s), n = \overline{1,N}\right\}, k = \overline{0,K-1}$$

The diagonal elements of the matrix $P_{k,k}$ are negative and, up to sign, determine the intensity of the exit of the Markovian chain ς_t, $t\geqslant 0$, from the corresponding state.

In the case where the number of requests in the queuing system is zero, the exit of the chain from the corresponding state can occur due to: – a change in the state of the controlling process of the incoming request flow (the intensity of such an event is characterized by the diagonal elements of matrix $diag\left\{B_0^{(n)}, n = \overline{1,N}\right\}$); – the change in a state of process n_t, $t\geqslant 0$, which characterizes the variability of the coverage area of the 5G cluster base station (the intensity of such an event is characterized by a diagonal elements of the matrix $G \otimes E_A$).

If a number of serviced requests k in the system is above zero, the exit of the Markovian chain ς_t, $t\geqslant 0$, from the corresponding state can also occur due to the transition of the controlling process of one of these requests (an intensity of such an event is characterized by the diagonal elements of the matrix $diag\left\{E_A \otimes D_k^{(n)}, n = \overline{1,N}\right\}$). However, if the number of incoming requests to the queuing system reaches K, the arrival of a new request at the system input, unaccompanied by a change in the state of the controlling process a_t, $t\geqslant 0$, does not cause a change in the state of process ς_t, $t\geqslant 0$, as such an incoming request is rejected. Therefore, we are interested in the difference that results from subtracting an intensity of the transition of a controlling process a_t, $t\geqslant 0$, to a same state, accompanied by request generation, from the total intensity of the queuing system exit from a corresponding state (an intensity of such an event is characterized by the diagonal elements of the matrix $diag\left\{B^{(n)} \otimes E_{J_K}, n = \overline{1,N}\right\}$).

A non-diagonal elements of a matrix $P_{k,k}$ characterize the intensities of transitions of the Markovian chain ς_t, $t\geqslant 0$, that are not accompanied by the change in a value of the component $k_t \in \{\overline{0,K}\}$, which represents the number of serviced requests in the 5G cluster. We refer to such transitions as: – the transition of the controlling process a_t, which is not accompanied by request generation (the intensity of such an event is characterized by a non-diagonal elements of a matrix $diag\left\{B_0^{(n)}, n = \overline{1,N}\right\}$); – the transition of process n_t, $t\geqslant 0$, which represents a variability of the coverage area of the 5G cluster base station (the intensity of such an event is characterized by the non-diagonal elements of matrix $G \otimes E_A$); – the transition of controlling process a_t, $t\geqslant 0$, which does not cause the termination of servicing any of the $k < K$ accepted requests (the intensity of such an event is characterized by the elements of matrix $diag\left\{E_A \otimes \Gamma_k\left(K,\Pi^{(n)}\right), n = \overline{1,N}\right\}$); – a transition of controlling process a_t, $t\geqslant 0$, resulting from a rejection of an incoming request because K requests are already being serviced in the 5G cluster (the intensity of such an event is characterized by a non-diagonal elements of matrix $diag\left\{B^{(n)} \otimes E_{J_K} n = \overline{1,N}\right\}$).

The elements of the matrix $P_{k,k-1}$, $k = \overline{1,K}$, characterize the intensities of transitions of the Markovian chain ς_t, $t\geqslant 0$, which result in a decrease in the number of serviced requests in the system by one. We refer to such transitions as: – a transition of controlling process a_t, $t\geqslant 0$, for one of a serviced requests to the first absorbing state, i.e., successful completion of servicing the corresponding request (the intensity of such an event is characterized by the elements of matrix $diag\left\{E_A \otimes \mathrm{B}_{K-k}\left(K,\widetilde{\Pi}_1^{(n)}\right), n = \overline{1,N}\right\}$); – a transition of controlling process a_t, $t\geqslant 0$, for one of a serviced requests to the second absorbing state, i.e., transitioning the corresponding request to handover mode (the intensity of such an event is characterized by the elements of matrix $diag\left\{E_A \otimes \mathrm{B}_{K-k}\left(K,\widetilde{\Pi}_2^{(n)}\right), n = \overline{1,N}\right\}$). By generalizing the aforementioned transition intensities in a format of block matrices, we obtain a generator $P_{k,k-1}$, $k = \overline{1,K}$, as provided in (3).

The elements of the matrix $P_{k,k+1}$, $k = \overline{0,K-1}$, characterize the intensities of transitions of the Markovian chain ς_t, $t\geqslant 0$, which increase a number of serviced requests in the system. Such an event occurs when the controlling process a_t, $t\geqslant 0$, transitions, accompanied by the arrival of an input request of type $s \in \{\overline{1,S}\}$ to the system (with a fixed state of the process n_t, $t\geqslant 0$, an intensity of such an event is characterized by the elements of the matrix $s = \overline{1,S}$), provided that the inequality $k < K$ is satisfied. The acceptance of an input request of type s by the system increases by one in a number of requests in a s–th service phase (the transition probabilities of the servicing process are characterized by the elements of the matrix $\mathrm{A}_k(b_s)$, provided that at the time of arrival of the new request, $k < K$ requests were being serviced in the system).

For computing the stationary distribution for the described queuing system, a robust and computationally efficient information technology is proposed, which generalizes the following steps:

Compute the matrix $H_1 = -P_{1,0}/H_{0,0}$;
Recursively compute the matrices H_k, $k = \overline{2,K}$: $H_k = -P_{k,k}/\left(P_{k-1,k-1} + H_{k-1}P_{k-2,k-1}\right)$;
Implementing inverse recursion to compute matrices H_k: $\mathrm{H}_K = E$, $\mathrm{H}_k = \mathrm{H}_{k+1}H_{k+1}$, $k = \overline{1,K}$;
Find the singular solution $\vec{q}_K$ of a system of equations $q_K\left(P_{K,K} + H_K P_{K-1,K}\right) = \vec{0}$, $q_0\sum_{k=0}^{K}\mathrm{H}_k\hat{\nu} = 1$;

Calculate the desired stationary probabilities $\vec{q}_k$, $k = \overline{1,K}$, as $\vec{q}_k = \vec{q}_K\mathrm{H}_k$, $k = \overline{0,K-1}$.

It's worth noting that all computational operations in the presented information technology are performed on non-negative matrices. This guarantees the stability of the information technology when implemented as a numerical method.

To enhance the clarity and transparency of the proposed information technology, we present its core logic in the form of structured pseudocode. This representation summarises the four-step recursive algorithm described above, highlighting the matrix-based construction of the generator components and the backward computation of stationary probability vectors.

Input:

- Generator matrix blocks $\mathrm{P}_{k,k-1}$; $\mathrm{P}_{k,k}$; $\mathrm{P}_{k,k+1}$ for all k = 0..K.
- Maximum number of simultaneous requests: K.
- Identity matrix E.

Output:

- Stationary probability vectors q_k for k = 0..K.

Step 1: Initialize recursion
H_1: = $-\mathrm{P}_{0,0}^{-1} \times \mathrm{P}_{0,1}$.
// Matrix H_1 maps q_1 from q_0 using the structure of P.
Step 2: Recursively compute H_2 … H_K.
For k = 2 to K:

H_k: = $-(P_{k,k} + P_{k,k-1} \times H_{k-1})^{-1} \times P_{k,k+1}$.
// Each H_k expresses q_k via q_0 through recursive dependencies.
Step 3: Compute vector q_K.
Solve:
q_K × P_K,K + q_K × H_K × P_K,K$_{-1}$ = 0.
and normalise: $\sum_k q_k = 1$.
// This gives the "top" stationary vector q_K as a base case.
Step 4: Compute remaining q_k.
For k = K–1 down to 0:
q_k: = q_{k + 1} × H_{k + 1}.
// Backward recursion retrieves full stationary distribution

2.3. Metric for evaluating the performance of an instance of the information and communication interaction process in a 5G cluster

Given the known values of the stationary probabilities $\vec{q}_k$, $k = \overline{0,K}$, it is possible to calculate the metric of performance indicators for an instance of the information and communication interaction process in a 5G cluster.

The average number of requests served in the 5G cluster will be determined by the expression

$$K_{srv} = \sum_{k=1}^{K} k\vec{q}_k\hat{v} \tag{4}$$

The intensity of the flow of serviced requests in the 5G cluster will be characterized by the expression

$$\lambda_+ = \sum_{k=1}^{K}\sum_{n=1}^{N} \vec{q}(k,n)\left(E_A \otimes \mathrm{B}_{K-k}\left(K, \widetilde{\Pi}_1^{(n)}\right)\right)\hat{v} \tag{5}$$

The intensity of the flow of requests accepted by the 5G base station, which changed the type to handover during the servicing process, will be characterized by the expression

$$\lambda_h = \sum_{k=1}^{K}\sum_{n=1}^{N} \vec{q}(k,n)\left(E_A \otimes \mathrm{B}_{K-k}\left(K, \widetilde{\Pi}_2^{(n)}\right)\right)\hat{v} \tag{6}$$

A probability of losing the incoming request due to exceeding the permissible connection timeout for the subscriber will be characterized by the expression

$$\mathrm{A}_{tmo} = \lambda_-/\eta \tag{7}$$

The probability of losing an incoming request from the s–th concentric sector of the coverage area of the base station, because the maximum number of requests is already being serviced in the 5G cluster, will be characterized by the expression

$$\mathrm{A}_{ovf}^{(s)} = \frac{1}{\eta_s}\sum_{n=1}^{N} \vec{q}(K,n)\left(B_s^{(n)} \otimes E_{J_K}\right)\hat{v}\frac{\partial^2\Omega}{\partial u \partial v}, s = \overline{1,S} \tag{8}$$

The probability of losing an incoming request because the maximum number of requests is already being serviced in the 5G cluster will be characterized by the expression

$$\mathrm{A}_{ovf} = \frac{1}{\eta}\vec{q}_K\left(\widetilde{B} \otimes E_{J_K}\right)\hat{v} = 1 - \frac{\lambda_+ + \lambda_h}{\eta} = \frac{1}{\eta}\sum_{s=1}^{S}\eta_s \mathrm{A}_{ovf}^{(s)} \tag{9}$$

The probability of losing any incoming request in an instance of a 5G cluster will be characterized by the expression

$$\mathrm{A}_{lst} = \mathrm{A}_{tmo} + \mathrm{A}_{ovf} = 1 - \lambda_+/\eta \tag{10}$$

Finally, the probability of completing the servicing of any request in an instance of a 5G cluster will be characterized by the expression

$$\mathrm{A}_+ = 1 - \mathrm{A}_{lst} \tag{11}$$

3. Results and discussion

The material of this section is focused on demonstrating the adequacy of the mathematical framework presented in the previous section and showcasing its functionality in solving practical tasks in the chosen subject area. By elucidating the functionality aspect, we have concentrated on depicting the relationship between the parameters of the model of information and communication interaction process in a 5G cluster and the state of the external stochastic process n_t, $t \geqslant 0$, which characterizes the variability of the coverage area of the base station. Furthermore, to demonstrate the flexibility of the proposed mathematical framework, we have investigated several relevant optimization tasks with a focus on controlled variables related to defining the metrics of performance indicators (4)-(11).

For our experiments, we selected an instance of a 5G cluster, within the coverage area of which three concentric sectors are designated: $S = 3$. We characterized the external stochastic process n_t, $t \geqslant 0$, with two states: $N = 2$, and defined the generator of the variability of the base station coverage area as $G = \begin{pmatrix} -0.0020 & 0.0020 \\ 0.0013 & -0.0013 \end{pmatrix}$. The probability that at any given moment the process n_t, $t \geqslant 0$, is in state $n = \{1,2\}$ is determined by set $p = \{0.3870, 0.6130\}$, accordingly.

Here and till the completion of the paragraph: for the fixed state of an external stochastic process $n = 1$, the flow of incoming requests reaching the base station of the 5G cluster from subscribers is characterized by matrices $B_0^{(1)} = \begin{pmatrix} -10 & 0 \\ 0 & -2 \end{pmatrix}$, $B_1^{(1)} = \begin{pmatrix} 9.15 & 0.05 \\ 0.013 & 0.405 \end{pmatrix}$, $B_2^{(1)} = \begin{pmatrix} 0.15 & 0.2 \\ 0.025 & 1.15 \end{pmatrix}$, $B_3^{(1)} = \begin{pmatrix} 0.5 & 0.05 \\ 0 & 0.5 \end{pmatrix}$. The intensity of this flow is denoted as $\eta^{(1)} = 2.912$, and the average intensities of request arrivals from the $s = \{1,2,3\}$–th concentric sector of the coverage area of the base station of the 5G cluster are represented by $\eta_1^{(1)} = 1.4167$, $\eta_2^{(1)} = 1.0901$, $\eta_3^{(1)} = 0.4046$. The coefficient of variation between the arrival intervals of incoming requests is denoted as $c_v = 1.645$, and the corresponding correlation coefficient is $c_r = 0.188$. The average duration of a subscriber's stay in the $s = \{1,2,3\}$–th concentric sector of the coverage area of the 5G cluster is denoted as $\{1/0.6, 1/0.5, 1/0.36\}$, accordingly. The probability of completing the servicing of a request of the $s = \{1,2,3\}$–th type is equal to $\{0.5/0.6, 2/3, 0.26/0.36\}$, respectively. The transition probabilities between concentric sectors $\{1\to2, 2\to1, 2\to3, 3\to2\}$ are represented by $\{0.1/0.6, 0.08/0.5, 0.08/0.5, 0.08/0.36\}$, accordingly. The probabilities of losing an incoming request due to exceeding the subscriber's waiting timeout for servicing requests of the $s = \{1,2,3\}$–th type are represented by $\{0.01/0.6, 0.01/0.5, 0.01/0.36\}$, respectively. A summary of all input parameters corresponding to the state n = 1n = 1 of the external stochastic process is provided in Table 2. This tabular representation consolidates the values of arrival intensities, service rates, transition probabilities, and loss probabilities across all coverage sectors.

For comparison, we now define the corresponding parameters for the alternative state $n = 2$ of the external stochastic process, which governs the variability of the base station's coverage area in the 5G cluster. For the fixed state of an external stochastic process $n = 2$, the flow of incoming requests reaching the base station of the 5G cluster from

Table 2
Model parameters for state $n = 1$ of the external stochastic process.

Sector s	$\eta_s^{(1)}$	$\lambda_s^{(1)}$	$\lambda_{s,+}^{(1)}$	$\lambda_{s,h}^{(1)}$	$\lambda_{s,-}^{(1)}$	$\lambda_{s,s'}^{(1)}$
1	1.4167	0.6	0.5	0.1	0.01	$\lambda_{1,2}^{(1)} = 0.1, \lambda_{1,3}^{(1)} = 0$
2	1.0901	0.5	0.35	0.08	0.01	$\lambda_{2,1}^{(1)} = 0.08, \lambda_{2,3}^{(1)} = 0.08$
3	0.4046	0.36	0.26	0.08	0.02	$\lambda_{3,1}^{(1)} = 0, \lambda_{3,2}^{(1)} = 0.08$

subscribers is characterized by matrices $B_0^{(2)} = \begin{pmatrix} -6.5 & 0 \\ 0 & -1 \end{pmatrix}$, $B_1^{(2)} = \begin{pmatrix} 0.6 & 0.05 \\ 0.013 & 0.27 \end{pmatrix}$, $B_2^{(2)} = \begin{pmatrix} 0.15 & 0.4 \\ 0.14 & 0.55 \end{pmatrix}$, $B_3^{(2)} = \begin{pmatrix} 5.3 & 0.05 \\ 0.01 & 0.005 \end{pmatrix}$. The intensity of this flow is denoted as $\eta^{(2)} = 2.412$, and the average intensities of request arrivals from the $s = \{1,2,3\}$−th concentric sector of the coverage area of the base station of the 5G cluster are represented by $\eta_1^{(2)} = 0.36376$, $\eta_2^{(2)} = 0.66631$, $\eta_3^{(2)} = 0.38335$. The coefficient of variation between the arrival intervals of incoming requests is denoted as $c_v = 2.75$, and the corresponding correlation coefficient is $c_r = 0.248$. The average duration of a subscriber's stay in the $s = \{1,2,3\}$−th concentric sector of the coverage area of the 5G cluster is denoted as $\{1/0.6, 1/0.2, 1/0.18\}$, accordingly. The probability of completing the servicing of a request of the $s = \{1,2,3\}$−th type is equal to $\{0.35/0.6, 0.13/0.2, 0.12/0.18\}$, respectively. The transition probabilities between concentric sectors $\{1\to2, 2\to1, 2\to3, 3\to2\}$ are represented by $\{0.06/0.6, 0.05/0.2, 0.05/0.2, 0.05/0.18\}$, accordingly. The probabilities of losing an incoming request due to exceeding the subscriber's waiting timeout for servicing requests of the $s = \{1,2,3\}$−th type are represented by $\{0.01/0.6, 0.01/0.2, 0.02/0.18\}$. respectively. Analogously, Table 3 presents the characteristic parameters for the state $n = 2$, facilitating a direct comparison between the two coverage configurations of the 5G base station under study.

A comparative analysis of the characteristic parameters corresponding to the two fixed states $n = 1$ and $n = 2$ of the external stochastic process reveals notable differences in the behaviour of subscriber-generated traffic. In particular, the total flow intensity decreases from $\eta^{(1)} = 2.912$ to $\eta^{(2)} = 2.412$, which is accompanied by a redistribution of request arrival intensities across the coverage sectors: the dominant sector shifts from $s = 1$ in state $n = 1$ to $s = 2$ in state $n = 2$. This structural transition is further reflected in the average service rates $\lambda_s^{(n)}$, where the service intensity in sector $s = 1$ decreases from 0.6 to 0.4, while that in sector $s = 3$ decreases more significantly from 0.36 to 0.18. Moreover, the probabilities of successful servicing $\lambda_{s,+}^{(n)}$ and loss probabilities $\lambda_{s,-}^{(n)}$ show a corresponding decline in efficiency under state $n = 2$, which is characterized by higher coefficient of variation $c_v = 2.75$ and increased correlation in request arrivals $c_r = 0.248$ compared to $c_v = 1.645$ and $c_r = 0.188$ in state $n = 1$. These variations illustrate the impact of the base station's coverage mode on the dynamics of subscriber interaction, justifying the consideration of both states in the stochastic model and their weighted contribution to the system's overall performance as reflected in the analytical expressions (5)-(10).

Let's demonstrate that the state of the external stochastic process n_t, $t \geqslant 0$, which characterizes the variability of the coverage area of the base station, indeed significantly influences the parameter values of the model of information and communication interaction processes in a 5G cluster. To do this, let's designate the aforementioned set of characteristic parameter values for an instance of a 5G cluster as ("taking into account External Conditions" or "+EC"). Instead, for the same instance of a 5G cluster, let's introduce a set of data whose characteristic parameters are determined without considering the influence of the external stochastic process n_t, $t \geqslant 0$. We'll identify this dataset as "without taking into account External Conditions" or "-EC". In fact, ignoring the process n_t, $t \geqslant 0$, simplifies the investigated model of a queuing system to one where three stationary Poisson request flows of type $s = \{\overline{1, S = 3}\}$ with intensities η_s are directed. These intensities are calculated by expression (1). The average intensities of transitions, movements, and request losses, in this case, are determined as the sums of products of the corresponding intensities values, defined above in the + EC set for the state of the external stochastic process $n = 1$, and probabilities p_1, and the products of the corresponding intensities values, defined above in the + EC set for the state of the external stochastic process $n = 2$, and probabilities p_2. For example, the average intensity of request loss due to the transition of the initiating subscriber from the second concentric sector of the coverage zone of the 5G cluster to the first is analytically characterized by the expression $\lambda_{2,1}^{(1)} p_1 + \lambda_{2,1}^{(2)} p_2$.

Table 3
Model parameters for state $n = 1$ of the external stochastic process.

Sector s	$\eta_s^{(1)}$	$\lambda_s^{(1)}$	$\lambda_{s,+}^{(1)}$	$\lambda_{s,h}^{(1)}$	$\lambda_{s,-}^{(1)}$	$\lambda_{s,s'}^{(1)}$
1	0.36376	0.4	0.35	0.04	0.01	$\lambda_{1,2}^{(2)} = 0.06, \lambda_{1,3}^{(2)} = 0$
2	0.66631	0.2	0.13	0.05	0.01	$\lambda_{2,1}^{(2)} = 0.05, \lambda_{2,3}^{(2)} = 0.05$
3	0.38335	0.18	0.12	0.04	0.02	$\lambda_{3,1}^{(2)} = 0, \lambda_{3,2}^{(2)} = 0.05$

Let's investigate how the values of quality indicators (4)-(11) depend on the number of information and communication interaction sessions K, supported by the base station of the 5G cluster. In the investigations, the results of which are presented below, we varied the value of K in the range of $[5, 50]$.

We calculate the dependencies of $K_{srv} = f(K)$ and $\lambda_+ = f(K)$ for the datasets + EC and −EC separately. The dependency of $K_{srv} = f(K)$, visualized in Fig. 2, demonstrates how the average number of requests served in an instance of a 5G cluster changes with increasing value of parameter K. This dependency was calculated using expression (4) based on the model defined for the investigated instance of the 5G cluster in form (3), determined using the information technology described at the end of Section 2.2. The dependency of $\lambda_+ = f(K)$, visualized in Fig. 3, demonstrates how the intensity of the flow of serviced requests in an instance of a 5G cluster changes with increasing value of parameter K. This dependency was calculated using expression (5).

Let's comment on the results presented in Figs. 2 and 3. It's worth noting that along the abscissa axis, we have values representing the capacity of the base station of the 5G cluster instance with established parameters, as mentioned at the beginning of the section. The capacity of the base station determines the maximum number of subscribers it can serve simultaneously. From Fig. 2, it's evident that for both datasets (−EC and + EC), an average number of serviced requests in a system reaches saturation (for dataset −EC at $K_{srv} = f(K = 25) = 11$, and for dataset + EC at $K_{srv} = f(K = 50) = 12$). The transition of these graphs into saturation mode can be explained by the fact that our presented model of information and communication interaction in the 5G cluster considers subscriber movements, which leads to request losses or their partial transfer to the handover mode, which is not counted as a successful completion of the servicing process for the target subscriber. Overall, the −EC model proved to be more sensitive than the + EC

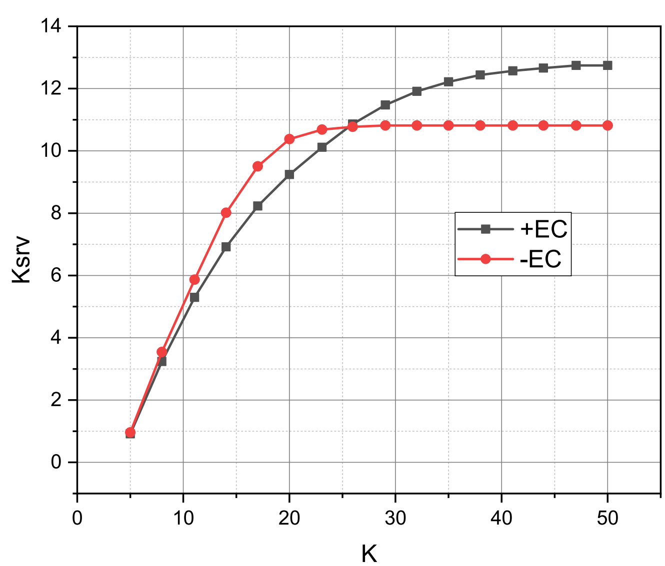

Fig. 2. Calculated dependence of $K_{srv} = f(K)$ for the + EC and −EC models, $n \in \{1, 2\}$, and $s = 0.75$.

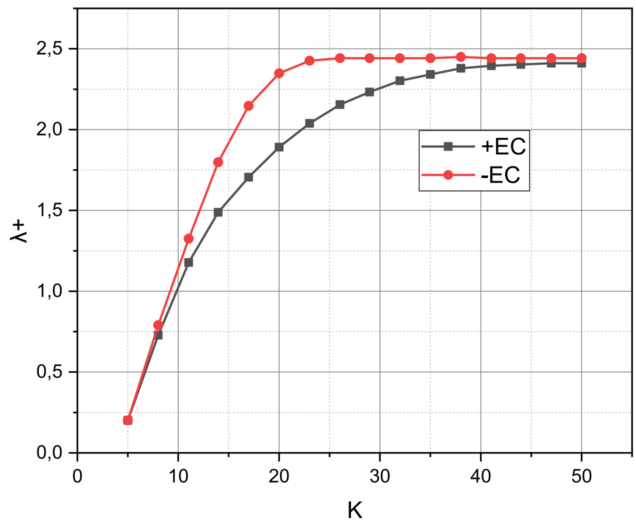

Fig. 3. Calculated dependence of $\lambda_+ = f(K)$ for the + EC and −EC models, $n \in \{1, 2\}$, and $s = 0.75$.

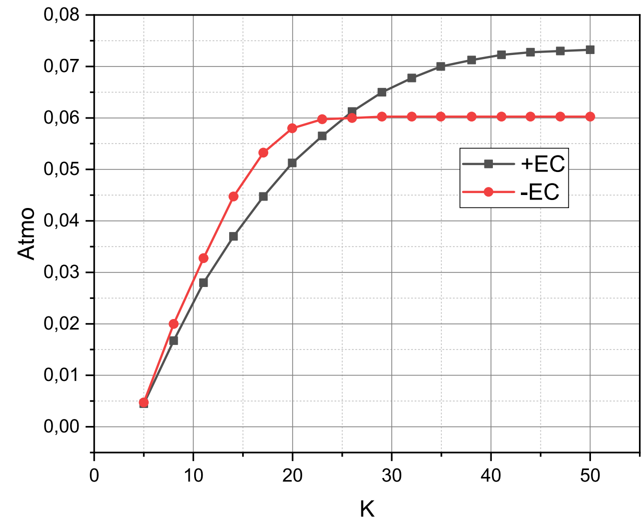

Fig. 5. Calculated dependence of $A_{tmo} = f(K)$ for the + EC and −EC models, and $s = 0.75$.

model. The data presented in Fig. 3 regarding the intensities of outgoing flows of successfully serviced requests for the −EC and + EC models correlate with the graphs presented in Fig. 3. Similarly, the −EC model reproduces the influence of the variability factor of the base station coverage area on the value of the quality indicator λ_+, which is functionally dependent on the value of the parameter K. This characterizes the adaptability quality of the −EC model to the real operating conditions of the investigated instance of the 5G cluster.

Now let's calculate the dependencies of $\lambda_h = f(K)$ and $A_{tmo} = f(K)$ for the datasets + EC and −EC separately. The dependency of $\lambda_h = f(K)$, visualized in Fig. 4, demonstrates how the intensity of the flow of requests accepted by the 5G base station, which changed their type to handover during servicing, changes with increasing value of the parameter K. This dependency was calculated using expression (6). The dependency of $A_{tmo} = f(K)$, visualized in Fig. 5, demonstrates how a probability of losing an incoming request due to exceeding the acceptable connection waiting timeout for the subscriber changes with increasing value of parameter K. This dependency was calculated using expression (7).

From the graphs shown in Fig. 4, it's evident that, according to the specified initial conditions, a significant number of accepted requests change their type to handover. This means that corresponding subscribers leave the coverage area of the 5G cluster before their initiated information and communication interaction processes are completed. This circumstance leads to the increase in ta number of lost requests in an investigated system. The graphs in Fig. 5 maintain the trend noted in Fig. 4. The probability of losing an incoming request due to exceeding the acceptable connection waiting timeout for the subscriber sensitively responds to the increase in the abscissa value until the probability A_{tmo} no longer depends on the value of parameter K. The −EC model allows for a clearer tracking of this moment.

Finally, let's calculate the dependencies of $A_{ovf} = f(K)$ and $A_{lst} = f(K)$ for the datasets +EC and −EC separately. The dependency of $A_{ovf} = f(K)$, visualized in Fig. 6, demonstrates how the probability of losing an incoming request because the maximum number of requests is already being serviced in an instance of the 5G cluster changes with increasing value of the parameter K. This dependency was calculated using expression (9). The dependency of $A_{lst} = f(K)$, visualized in Fig. 7, demonstrates how the probability of losing any incoming request in an instance of the 5G cluster changes with increasing value of the parameter K. This dependency was calculated using expression (10).

The results presented in Fig. 6 allow us to track the moment when the value of the parameter K ceases to influence the probability of losing an

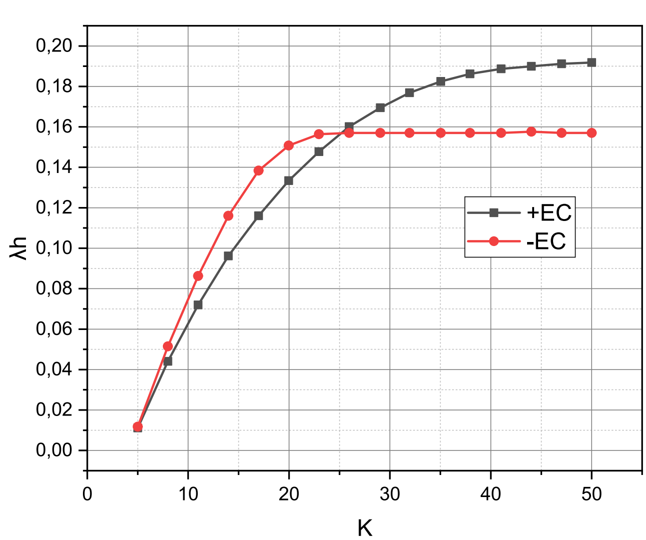

Fig. 4. Calculated dependence of $\lambda_h = f(K)$ for the + EC and −EC models.

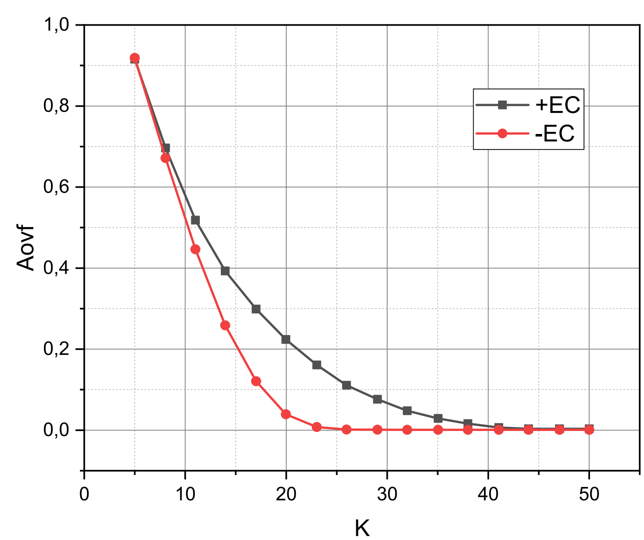

Fig. 6. Calculated dependence of $A_{ovf} = f(K)$ for the + EC and −EC models.

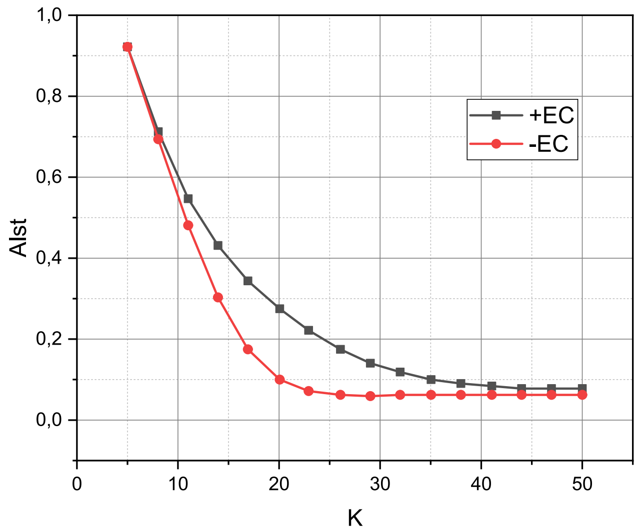

Fig. 7. Calculated dependence of $A_{lst} = f(K)$ for the + EC and −EC models.

incoming request because the maximum number of requests is already being serviced in an instance of the 5G cluster. The qualitative parameter A_{ovf} has a direct economic interpretation, as the number of subscribers that can be simultaneously serviced in a designed 5G cluster is one of the primary characteristics of such systems. It's worth noting the accuracy of the model, which takes into account the influence of the external stochastic process n_t, $t \geqslant 0$, on the value of the quality indicator A_{ovf}. Thanks to this model, we see that for the given saturation conditions, the saturation of the dependency $A_{ovf} = f(K)$ graph is achieved at $K = 26$, not at 43. Thus, it's possible to reduce the costs for the capacity of radio equipment of the designed 5G cluster by almost half. The graphs from Fig. 7 show that the unspecified (generalized) probability of losing any incoming request in an instance of the 5G cluster is largely determined by the capacity value K: the final probability A_{ovf} after the graphs reach saturation at $A_{ovf} = f(K)$ does not exceed 0.005.

Overall, the data presented in Figs. 2-7 indicates that the values of the quality indicators (4)-(7), (9), (10) are sensitive to the correlation between the incoming request flow and the flow that characterizes the variability of the coverage area of the base station of the 5G cluster. The values of all evaluated quality characteristics, including the average intensities of arrival, service, movement, and loss of requests, determined for the −EC dataset, turned out to be better than the values of similar quality parameters determined for the + EC dataset. Therefore, considering the variability of the coverage area of the base station of the 5G cluster is advisable when designing real systems for the corresponding purpose.

From a computational standpoint, the proposed model demonstrates favourable characteristics in terms of both time and space complexity. The underlying continuous-time Markov chain has a multidimensional structure, where the size of the state space increases linearly with the number of concurrent sessions K and the number of service sectors $S = 3$. Due to the sparsity and regularity of the generator matrix Q, the number of non-zero elements grows proportionally to $O(KS^2)$, which ensures efficient memory usage and facilitates scalable matrix operations. The stationary probability vector $\overrightarrow{\pi}$ is computed by solving the linear system $\overrightarrow{\pi} Q = \overrightarrow{0}$, subject to the normalisation constraint $\sum_i \pi_i = 1$. This is accomplished using an iterative numerical method, such as the power method or Gauss–Seidel iteration. For the values of K used in the numerical experiments ($K \leqslant 15$), convergence is typically reached within 40–50 iterations, each requiring computational effort proportional to $O(KS^2)$. As a result, the overall complexity of evaluating the system's performance indicators—including those defined by expressions (5)-(10) – remains polynomial in K and manageable for real-time performance analysis in high-loaded 5G-IoT clusters. The analytical tractability and structured sparsity of the proposed approach offer distinct advantages over simulation-based techniques, particularly in terms of repeatability, scalability, and integration with optimisation workflows.

As emphasized at the beginning of the section, based on the mathematical apparatus presented in the article, the generalization of the metric of qualitative indicators (4)-(10) allows the formulation of various optimization tasks depending on the specific application of the 5G cluster instance. For instance, an optimization task involves determining the minimum capacity K of the 5G cluster's base station necessary to ensure that the request loss probability does not exceed 0.2. Fig. 7 shows that for the instance of the 5G cluster, whose model does not consider the variability of the base station coverage zone (−EC), the sought solution to such an optimization problem is $K = 16$. Meanwhile, for the qualitative indicator hh value $K = 16$ for the 5G cluster instance whose model takes into account the variability of the base station coverage zone (+EC), it equals 0.39, meaning that in real operational conditions, the actual value of A_{lst} will practically exceed the design value by almost twice (0.2). To achieve the design value $A_{lst} = 0.2$ of the 5G cluster instance represented by the "+EC" model, it is necessary to operate with the parameter K at the level of 24.

4. Conclusions and future work

In this study, we developed a stochastic model to analyse the information and communication interaction between a base station and a set of subscribers in a 5G cluster with variable coverage zones. The model was formalised as a multidimensional Markovian queuing system, where the dynamics of the base station's coverage area were governed by an external two-state stochastic process. This approach enabled the incorporation of realistic environmental and traffic variability into the system analysis.

We derived a set of analytical expressions (formulas (5)-(10)) for key performance metrics, including the average intensity of successfully serviced requests, the blocking and loss probabilities, and the average number of active sessions in each coverage sector. These expressions were obtained based on the stationary distribution of the underlying Markov chain, providing a computationally efficient mechanism for performance evaluation.

The numerical experiment, conducted using representative input parameters for each state of the external process, revealed several important findings:

- The performance of the 5G cluster is sensitive to changes in request arrival and service rates, particularly under the influence of external state transitions.
- The shift in dominant traffic sectors between states $n = 1$ and $n = 2$ leads to measurable rebalancing in resource utilisation across the coverage area.
- Increasing the number of simultaneous sessions K improves performance metrics up to a threshold beyond which diminishing returns are observed.

An important contribution of the proposed model is the availability of closed-form analytical expressions for system-level indicators, which contrasts with simulation-based approaches typically used in the analysis of dynamic 5G environments. This feature allows for parameter sensitivity studies and rapid system evaluation without requiring costly simulations.

The proposed framework can be applied to the planning and optimisation of 5G-IoT networks in real-world scenarios with highly dynamic user behaviour, such as urban mobility environments, industrial automation zones, or public infrastructure clusters. By capturing state-dependent traffic and service characteristics, the model offers insights into how adaptive coverage policies and session concurrency limits impact system performance.

Future research may address the integration of queuing systems with buffer constraints, the use of non-exponential service time distributions, and the extension of the external stochastic process to more than two states. Furthermore, incorporating real-time radio resource scheduling mechanisms—such as NR-Scheduling algorithms and frequency hopping schemes in unlicensed 5G bands—would enhance the model's applicability to advanced 5G and beyond-5G deployments.

CRediT authorship contribution statement

Viacheslav Kovtun: Writing – review & editing, Visualization, Investigation, Conceptualization, Software, Supervision, Project administration, Writing – original draft, Methodology, Formal analysis. **Oksana Kovtun:** Writing – review & editing, Visualization, Resources, Writing – original draft, Validation, Project administration, Data curation, Investigation, Conceptualization. **Jamil Abedalrahim Jamil Alsayaydeh:** Validation, Data curation, Writing – review & editing, Resources.

Funding

This research is part of the project No. 2022/45/P/ST7/03450 co-funded by the National Science Centre and the European Union Framework Programme for Research and Innovation Horizon 2020 under the Marie Skłodowska-Curie grant agreement No. 945339. For the purpose of Open Access, the author has applied a CC-BY public copyright licence to any Author Accepted Manuscript (AAM) version arising from this submission.

Declaration of competing interest

The authors declare that they have no known competing financial interests or personal relationships that could have appeared to influence the work reported in this paper.

Acknowledgments

The authors are grateful to all colleagues and institutions that contributed to the research and made it possible to publish its results.

References

[1] Cainelli GP, Underberg L. Performance testing of a 5G campus network in real-world propagation conditions from the application's point of view. IFAC-PapersOnLine 2023;56(2):9837–42. https://doi.org/10.1016/j.ifacol.2023.10.404.

[2] Chan Y-C, Wu J, Wong EWM, Leung CS. Integrating teletraffic theory with neural networks for quality-of-service evaluation in mobile networks. Appl Soft Comput 2024;152:111208. https://doi.org/10.1016/j.asoc.2023.111208.

[3] Elimadi M, Abbas-Turki A, Koukam A, Dridi M, Mualla Y. Review of traffic assignment and future challenges. Appl Sci 2024;14(2):683. https://doi.org/10.3390/app14020683.

[4] Kovtun V, Grochla K, Altameem T, Al-Maitah M. Evaluation of the QoS policy model of an ordinary 5G smart city cluster with predominant URLLC and eMBB traffic. PLOS ONE 2023;18(12):e0295252. https://doi.org/10.1371/journal.pone.0295252.

[5] Adil M, Song H, Khan MK, Farouk A, Jin Z. 5G/6G-enabled metaverse technologies: taxonomy, applications, and open security challenges with future research directions. J Network Comp Appl 2024;223:103828. https://doi.org/10.1016/j.jnca.2024.103828.

[6] Kovtun V, Izonin I, Gregus M. Formalization of the metric of parameters for quality evaluation of the subject-system interaction session in the 5G-IoT ecosystem. Alexandria Eng J 2022;61(10):7941–52. https://doi.org/10.1016/j.aej.2022.01.054.

[7] Du A. Implications of 5G rollout on post-earthquake functionality of regional telecommunication infrastructure. J Infrastruct Intellig Resilience 2024;3(1):100084. https://doi.org/10.1016/j.iintel.2024.100084.

[8] Kumar A, et al. Evaluation of 5G techniques affecting the deployment of smart hospital infrastructure: understanding 5G, AI and IoT role in smart hospital. Alexandria Eng J 2023;83:335–54. https://doi.org/10.1016/j.aej.2023.10.065.

[9] Kovtun V, Grochla K, Połys K. The concept of network resource control of a 5G cluster focused on the smart city's critical infrastructure needs. Elsevier BV Alexandria Eng J May 2024;94:248–56. https://doi.org/10.1016/j.aej.2024.03.038.

[10] Rochman MI, et al. A comprehensive analysis of the coverage and performance of 4G and 5G deployments. Elsevier BV Comp Networks Dec. 2023;237. https://doi.org/10.1016/j.comnet.2023.110060.

[11] Kousias K, et al. Empirical performance analysis and ML-based modeling of 5G non-standalone networks. Elsevier BV Comp Networks Mar. 2024;241. https://doi.org/10.1016/j.comnet.2024.110207.

[12] Gallego-Madrid J, Molina-Zarca A, Sanchez-Iborra R, Ortiz J, Skarmeta AF. Fast traffic processing in multi-tenant 5G environments: a comparative performance evaluation of P4 and eBPF technologies. Eng Sci Tech, Int J Apr. 2024;52. https://doi.org/10.1016/j.jestch.2024.101678.

[13] Liu P, et al. Towards 5G new radio sidelink communications: a versatile link-level simulator and performance evaluation. Elsevier BV Comp Commun Aug. 2023;208:231–43. https://doi.org/10.1016/j.comcom.2023.06.005.

[14] Fiandrino C, Martínez-Villanueva DJ, Widmer J. A study on 5G performance and fast conditional handover for public transit systems. Elsevier BV Comp Commun Sep. 2023;209:499–512. https://doi.org/10.1016/j.comcom.2023.07.020.

[15] Usman Hadi M. Towards optimization of 5G NR transport over fiber links performance in 5G Multi-band Networks: an OMSA model approach. Opt Fiber Tech 2023;79:103358. https://doi.org/10.1016/j.yofte.2023.103358.

[16] Mathur S, Chaba Y, Noliya A. Performance analysis of support vector machine learning based carrier aggregation resource scheduling in 5G mobile communication. Elsevier BV Procedia Comp Sci 2023;218:2776–85. https://doi.org/10.1016/j.procs.2023.01.249.

[17] Alotaibi AA, AlQahtani SA. Performance analysis in overlay-based cognitive D2D communications in 5G networks. Elsevier BV J King Saud Univ - Comp Info Sci Jul. 2023;35(7). https://doi.org/10.1016/j.jksuci.2023.101599.

[18] Liu P, et al. Towards 5G new radio sidelink communications: a versatile link-level simulator and performance evaluation. Elsevier BV Comp Commun Aug. 2023;208:231–43. https://doi.org/10.1016/j.comcom.2023.06.005.

[19] Ansari J, et al. Performance of 5G trials for industrial automation. Electronics 2022;11(3):412. https://doi.org/10.3390/electronics11030412.

[20] Saleh S, Saeidi T, Timmons N, Razzaz F. A comprehensive review of recent methods for compactness and performance enhancement in 5G and 6G wearable antennas. Elsevier BV Alexandria Eng J May 2024;95:132–63. https://doi.org/10.1016/j.aej.2024.03.097.

[21] Cicioğlu M. Performance analysis of handover management in 5G small cells. Elsevier BV Comp Stand Interfaces Apr. 2021;75. https://doi.org/10.1016/j.csi.2020.103502.

[22] Islam S, Budati AK, Hasan MK, Goyal SB, Khanna A. Performance analysis of video data transmission for telemedicine applications with 5G enabled Internet of Things. Elsevier BV Comp Elect Eng May 2023;108. https://doi.org/10.1016/j.compeleceng.2023.108712.

[23] Azimi Y, Yousefi S, Kalbkhani H, Kunz T. Mobility aware and energy-efficient federated deep reinforcement learning assisted resource allocation for 5G-RAN slicing. Elsevier BV Comp Commun Mar. 2024;217:166–82. https://doi.org/10.1016/j.comcom.2024.01.028.

[24] Siahpoosh SAA, Rezaei F. A study on the impact of mobility on caching in non-standalone 5G vehicular networks. Elsevier BV Vehicular Commun Jun. 2023;41. https://doi.org/10.1016/j.vehcom.2023.100595.

[25] Jain A, Lopez-Aguilera E, Demirkol I. Are mobility management solutions ready for 5G and beyond?. Elsevier BV Comp Commun Sep. 2020;161:50–75. https://doi.org/10.1016/j.comcom.2020.07.016.

[26] Palas MdR, et al. Multi-criteria handover mobility management in 5G cellular network. Elsevier BV Computer Communications Jun. 2021;174:81–91. https://doi.org/10.1016/j.comcom.2021.04.020.

[27] Akkari N, Dimitriou N. Mobility management solutions for 5G networks: architecture and services. Elsevier BV Comp Networks Mar. 2020;169. https://doi.org/10.1016/j.comnet.2019.107082.

[28] Roy P, Tahsin A, Sarker S, Adhikary T, Razzaque MdA, Hassan MM. User mobility and quality-of-experience aware placement of virtual network functions in 5G. Elsevier BV Comp Commun 2020;150:367–77. https://doi.org/10.1016/j.comcom.2019.12.005.

[29] Chen Z, Tang J, Zhang XY, So DKC, Jin S, Wong K-K. Hybrid evolutionary-based sparse channel estimation for IRS-assisted mmWave MIMO systems. Institute of Electrical and Electronics Engineers (IEEE) IEEE Trans Wireless Commun 2022;21(3):1586–601. https://doi.org/10.1109/twc.2021.3105405.

[30] Zhu L, Zhang J, Xiao Z, Cao X, Wu DO, Xia X-G. 3-D Beamforming for flexible coverage in millimeter-wave UAV communications. Institute of Electrical and Electronics Engineers (IEEE) IEEE Wireless Commun Lett 2019;8(3):837–40. https://doi.org/10.1109/lwc.2019.2895597.

[31] Acal C, Ruiz-Castro JE, Maldonado D, Roldán JB. One cut-point phase-type distributions in reliability. an application to resistive random access memories. MDPI AG Mathematics 2021;9(21):2734. https://doi.org/10.3390/math9212734.

[32] Medhi J. "Miscellaneous Topics," Stochastic Models in Queueing Theory. Elsevier 2003:375–468. https://doi.org/10.1016/b978-012487462-6/50008-4.

VIACHESLAV KOVTUN received the Ph.D. degree in information and measuring systems in 2006, the Dr.Sc. degree in information technologies in 2021, and Dr.Hab. degree in computer science and telecommunications in 2023. He is currently a Head of the Computer Control Systems Department at Vinnytsia National Technical University, Ukraine. His main research interests include system analysis, information technologies, machine learning, pattern recognition, and signal processing.

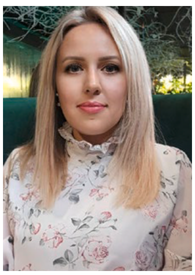

OKSANA KOVTUN, associate professor of the Department of theory and practice of translation of Vasyl' Stus Donetsk National University, received the Ph.D. degree in philology in 2012 and is currently working on a doctoral in the specialty of comparative and contrastive linguistics. She authored over 90 research papers. Her scientific interests are linguistics, grammar, contrastive grammar, methods of language teaching, computational linguistics, translation studies, lingua axiology, communicative linguistics, discourse linguistics, gender linguistics, sociolinguistics, lexicography, phraseography.

JAMIL ABEDALRAHIM JAMIL ALSAYAYDEH (Member, IEEE) received a degree in computer engineering from Zaporizhzhya National Technical University, Ukraine, in 2009, an M.S. degree in computer systems and networks from Zaporizhzhya National Technical University, Ukraine, in 2010 and Ph.D in Engineering Sciences with a specialization in Automation of Control Processes from National Mining University, Ukraine, in 2014. He is currently a Senior Lecturer at the Department of Engineering Technology, Faculty of Electronic and Computer Engineering and Technology, Universiti Teknikal Malaysia Melaka (UTeM) since 2015. His teaching portfolio includes a range of courses such as Computer Network & Security, Internet Technology & Multimedia, Software Engineering, Computer System Engineering, Data Communications & Computer Network, Computer Network & System, Real Time System, Programming Fundamental, Digital Signal Processing, Advanced Programming. He is a research member at Center for Advanced Computing Technology, his research interests are formal methods, simulation, Internet of Things, Computing Technology, Artificial Intelligence and Machine Learning: Computer Architecture, Algorithms, and Applications, Dr. Alsayaydeh has more than 57 research publications to his credit that are indexed in SSCI, SCIE, and Scopus, which cited by over 220 documents. He supervised undergraduate and postgraduate students and he is a reviewing member of various reputed journals. Currently he actively publishes research articles, received grants from the government and private sectors, universities and international collaboration. He is also as a Member of Board of Engineers Malaysia (BEM). He can be contacted at email: jamil@utem.edu.my.